In-Situ Second-Harmonic Generation and Luminescence Measurements for Structural Characterization of Ruthenium−Polypyridine Complex Monolayers with Two and Four Aliphatic Tails at the Air/Water Interface

Takashi Nakano, Yasuhiro Yamada, Taku Matsuo, and Sunao Yamada*

Department of Materials Physics and Chemistry, Kyushu University, Hakozaki, Higashi-ku, Fukuoka 812-8581, Japan

Received: July 15, 1998

Langmuir monolayer assemblies of ruthenium−polypyridine complexes having two and four aliphatic tails were studied by in-situ optical second-harmonic generation (SHG) and luminescence measurements, together with surface pressure−molecular area (π−A) isotherms. As the monolayer was compressed, the four-tailed complex showed a distinct phase transition at a 30−40 mN/m region from phase I (1.3 nm^2 mean molecular area) to phase II (1.1 nm^2). Excitation with 1064-nm light gave an SHG signal at 532 nm that appeared almost synchronously with the increase of surface pressure, but the p-polarized component of the SHG signal, induced by either p- (parallel to the plane of incidence) or s- (perpendicular to the plane of incidence) polarized fundamental light, showed a different profile upon compression of the monolayer. In the phase II region, the p-polarized component increased steeply, whereas the s-polarized component decreased to almost zero. A significant blue-shift and a longer lifetime of the luminescence signal were also observed in phase II. Thus, a tightly packed structure in which the main hyperpolarizability tensor is directed roughly perpendicular to the water surface is suggested for phase II. For the two-tailed complex, on the other hand, no appreciable phase transitions were observed, only a liquid-expanded phase (0.9 nm^2). The results are ascribed to differences in the number of long aliphatic tails.

Introduction

Much interest has been given to organic monolayer assemblies at the air/water interface, because of their promising applications to molecular devices as Langmuir−Blodgett (LB) films. A variety of spectroscopic techniques have been used to characterize monolayer assemblies at the air/water interface.[1] Surface second-harmonic generation (SHG) spectroscopy is sensitive for investigating molecular orientation at surfaces (interfaces), because surface SHG occurs only in electronically noncentrosymmetric moieties.[2−5] With this technique, the orientations of several amphiphilic dyes at the air/water interface have been investigated as a function of surface pressure (or surface number density).[2−13] Fluorescence spectroscopy is also sensitive to orientation effects and has been successful in studying the structure of and dynamics of monolayer assemblies in which charge-transfer and other intermolecular interactions occur.[13] Thus, the combination of SHG and fluorescence spectroscopy offers much useful information for structural characterization of monolayer assemblies at the air/water interface.

Ruthenium tris(2,2′-bipyridine) homologues are excellent photosensitizers for artificial photosynthesis systems and for optoelectronic devices, so the construction of thin films based on these materials is attractive. We have previously reported SHG responses from an LB monolayer assembly of a ruthenium tris(2,2′-bipyridine) homologue, Ru2C16B.[14] Since this type of ruthenium complex has a molecular hyperpolarizability of 70×10^{-30} esu (based on metal-to-ligand charge-transfer transition) and is stable against light irradiation,[15] applications to nonlinear optical devices are also interesting. The surface SHG technique can therefore be applied for investigating the ordering of monolayer structure for this type of ruthenium complex.

CHART 1

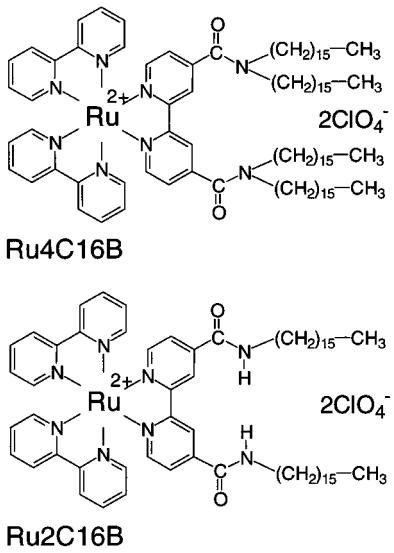

In this paper, we report significant differences in the monolayer structures of two amphiphilic ruthenium tris(2,2′-bipyridine) homologues, Ru2C16B and Ru4C16B (see Chart 1) having two and four aliphatic tails, respectively, as studied by in-situ SHG and luminescence measurements.

Experimental Section

Materials. Both amphiphilic ruthenium (II) polypyridine complexes were synthesized in our laboratory. The ruthenium

* Author for correspondence. E-mail: sunaotcm@mbox.nc.kyushu-u.ac.jp.

10.1021/jp983028u CCC: $15.00
Published on Web 10/03/1998

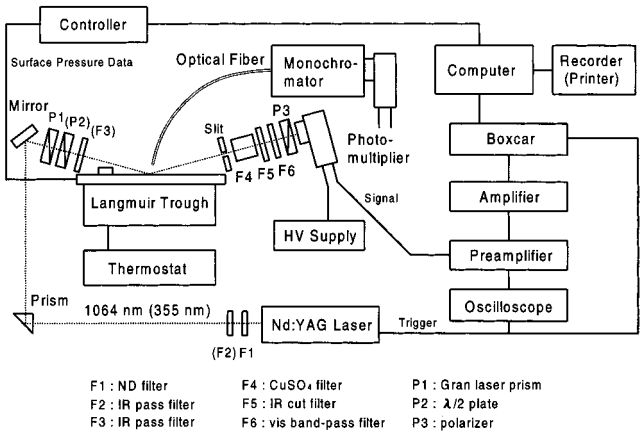

Figure 1. Experimental setup for SHG and luminescence signal measurements at an air/water interface: optical alignment for SHG measurements by 1064-nm laser radiation is shown. In the case of luminescence measurements using 355-nm radiation, P2, F2, and F3 (shown in parentheses) are removed and the mirror for 355-nm reflection is used.

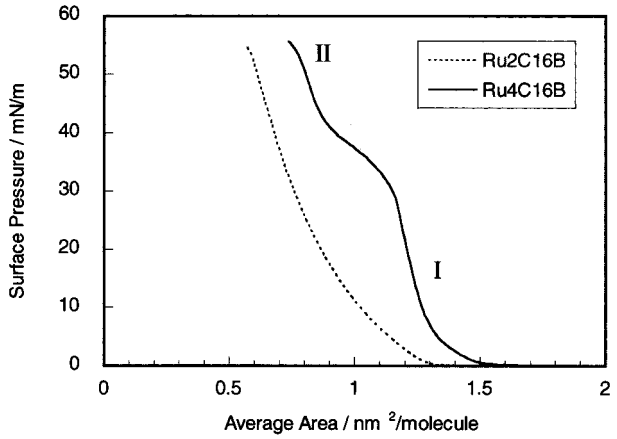

Figure 2. Surface pressure−Area ($\pi-A$) isotherms (293 K) of Ru4C16B and Ru2C16B. Compression speed is 20 mm/min.

complex with four *n*-hexadecyl groups (Ru4C16B) was prepared in a similar manner as the ruthenium complex with two *n*-hexadecyl groups (Ru2C16B).[16] As the first step, *N*,*N*,*N*′,*N*′-tetra(*n*-hexadecyl)-2,2′-bipyridine-4,4′dicarboxamide (4C16B) was obtained by the reaction of 2,2′-bipyridine-4,4′-dicarboxyl chloride and di(*n*-hexadecyl)amine; it was well soluble in various organic solvents. Recrystallization from hexane gave a colorless powder (17%): mp 80.5−81.5°. The corresponding ruthenium complex, Ru4C16B, was prepared by the reaction of 4C16B and bis(2,2′-bipyridine)ruthenium(II) in ethanol. The crude product was recrystallized from ethanol−water (4:1) containing excess $NaClO_4$. Found: C, 65.40%; H, 8.87%; N, 6.37%. Calcd. for $C_{96}H_{170}Cl_2N_8O_{10}Ru$: C, 65.20%; H, 9.68%; N, 6.33%.

SHG and Luminescence Measurements. The experimental setup for SHG and luminescence signal measurements is shown in Figure 1. In the case of second-harmonic (SH) signal measurements, pulses at the fundamental wavelength (1064 nm) from a Nd:YAG laser (Continuum Surelite-I, pulse duration 5−7 ns, 10 Hz) were p- (parallel to the plane of incidence) or s- (perpendicular to the plane of incidence) polarized by using a Gran laser prism (P1) and a half-wavelength plate (P2). The p- or s-polarized fundamental light (∼40 mJ/pulse) irradiated the water surface at an incident angle of 75° without focusing. The reflected SH light (532 nm) was detected by a photomultiplier (Hamamatsu R1477) through appropriate filters (F4−F6) and a polarizer (P3) to detect the polarized SH signal. The signal was amplified by a preamplifier (NF BX-31), and the amplified signal was averaged by a boxcar integrator (NF BX-531). In each signal measurement, the laser was operated at a repetition rate of 10 Hz, and the SH signal at 532 nm, obtained by integration over 32 laser pulses, was measured continuously both during compression of the monolayer film and at a constant surface pressure.

The third-harmonic light (355 nm) of the Nd:YAG laser (10 mJ/pulse, 4−6 ns) was used as an excitation light source at the same incident angle, by removing unwanted optics (F2, P2, F3) and replacing the mirror for 355-nm laser reflection. The luminescence signal was collected by an optical fiber cable (SIGMA KOKI MSL-1500F), one end of which was fixed just above the irradiation position (∼1 cm from the water surface). The other end of the fiber was connected to a monochromator (Jobin Yvon H-20), and the luminescence signal was detected by the photomultiplier, signal acquisition being the same as for the SHG measurements. The luminescence lifetime at 660 nm was obtained by integration over 32 laser pulses with a digital storagescope (Iwatsu DS-8621). Surface pressures were kept constant during the luminescence measurements.

A standard Langmuir trough (400 × 100 mm, USI Co. Ltd.) equipped with a film balance controller (USI System FSD-110) for measuring surface pressure was used. Water was deionized with a Milli-Q system (Millipore). The ruthenium complex (30 μl, 0.03 μmol) was spread from a chloroform solution (1 mM) onto a water subphase. The surface pressure−molecular area ($\pi-A$) isotherm was measured at a compression speed of 20 mm/min (corresponding to 0.11 nm^2 $molecule^{-1}$ min^{-1}) and at a controlled temperature of 293 K.

Results and Discussion

The amphiphilic property of the present ruthenium complexes is based on the hydrophilic headgroup and hydrophobic *n*-hexadecyl groups bound to one of the bipyridine ligands via amide bonds. This should also make the metal-to-ligand charge-transfer (MLCT) transition asymmetric, responsible for the second-order nonlinear optical response. As shown in Figure 2, the $\pi-A$ isotherm of Ru4C16B displayed a distinct phase transition in the ∼30 to ∼40 mN/m (∼1.2 to ∼0.95 nm^2 $molecule^{-1}$) region; the extrapolated mean molecular areas for phases I and II (see Figure 2) were 1.3 and 1.1 nm^2, respectively. This phase-transition isotherm was clearer at lower water temperatures.

According to the Corey−Pauling−Koltun molecular model, the cross-section of the hydrophilic headgroup is 0.8−0.9 nm^2 $molecule^{-1}$, that of a *n*-hexadecyl group is 0.2 nm^2 $molecule^{-1}$. Thus, the observed value (1.1 nm^2 $molecule^{-1}$) for the phase II structure seems reasonable, if the four *n*-hexadecyl groups are aligned tightly by hydrophobic effects. In the phase I structure, some of *n*-hexadecyl groups may be less aligned than is estimated from the molecular model.

As described above, an electronic transition from the metal to the bipyridine ligand having two amide groups is responsible for the SHG of the Ru4C16B complex. In fact, reflected SHG signals were clearly observed from the monolayer assembly of the ruthenium complex at the water surface. The p-polarized component of reflected SH light induced by p- or s-polarized fundamental light, denoted as I_{p-p} or I_{s-p}, was measured together with the $\pi-A$ isotherm.

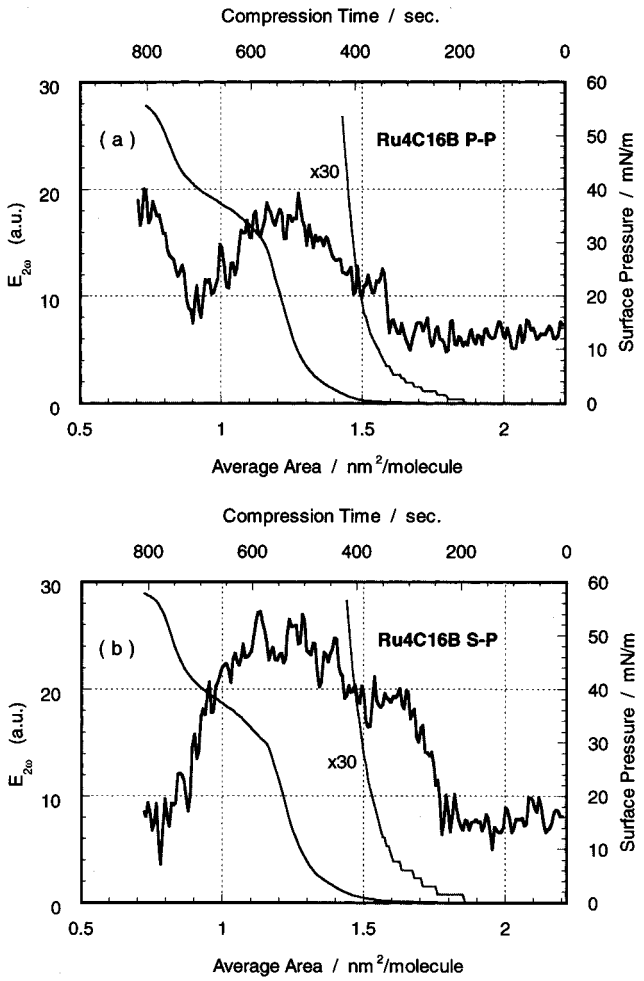

Figure 3. Relationships between SH field ($E_{2\omega}$) and molecular area (A), and $\pi-A$ isotherm for Ru4C16B. A part of $\pi-A$ isotherm is magnified for clarify. Polarized components of SH field: (a) p−p, (b) s−p.

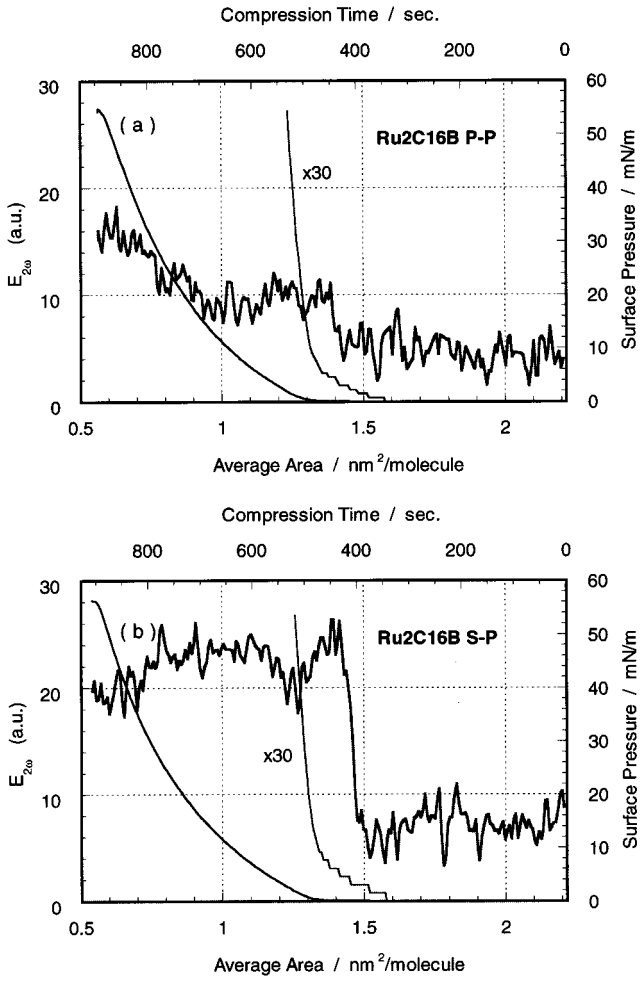

Figure 4. Relationships between SH field ($E_{2\omega}$), molecular area (A), and $\pi-A$ isotherm for Ru2C16B. A part of $\pi-A$ isotherm is magnified for clarity. Polarized components of the SH field: (a) p−p, (b) s−p.

If one assumes that all of the SHG-active molecules adsorbed to the water surface align in the same direction, the intensity of the SHG signal will be proportional to the square of the concentration of molecules. Thus, the SH field $E_{2\omega}$ (square root of SHG signal intensity) has been frequently used to monitor the relative coverage of SHG-active molecules.[2−5]

As shown in Figure 3a and 3b, the SHG signal tended to increase almost at the same time as the surface pressure increased, but each polarized component showed a different dependence on surface pressure. As shown in Figure 3a, the I_{p-p} component increased with increasing surface pressure in the region of phase I. In the please-transition region however, it decreased to nearly zero but increased again steeply with additional compression in the region of phase II. The I_{s-p} component rose rather steeply and increased with continuing compression in the region of phase I, and then decreased to zero in the phase-transition region; however, the signal did not increase again even with further compression (Figure 3b). The signal at the zero surface-pressure region may be the background value (scattered and stray lights, and electrical noise) because it was observed even from the water surface. Although the p-polarized SH components were clearly observed, as shown in Figures 3 and 4, no appreciable s-polarized SH components were detected, that is, the s-polarized component of molecular hyperpolarizability is negligible. Thus, the results suggest C∞v symmetry for the average molecular hyperpolarizability in the monolayer.

The average tilt angle Θ of the second-order molecular hyperpolarizability by the projection model[6,7,17] is evaluated from the ratio of p-polarized SH signals, I_{p-p}/I_{s-p}, as:

$$I_{p-p}/I_{s-p} = (\chi_{//} \sin^3\theta - \chi_{\perp} \sin\theta \cos^2\theta)^2/(\chi_{\perp} \sin\theta)^2$$

$$\tan 2\Theta = 2\,(\chi_{\perp}/\chi_{//})$$

where $\chi_{//}$ and $\chi_{\perp}$ stand for second-order nonlinear susceptibility tensors parallel and perpendicular to the surface normal, respectively, and θ is an incident angle of the laser light.[17] Thus, I_{p-p}/I_{s-p} (or its square root) is indicative of the direction of molecular hyperpolarizability. It therefore appears that some ordered alignments of Ru4C16B are established in phase I under the restriction of molecular motion but then deteriorate in the phase-transition region. Since the I_{p-p} component increased steeply, while the I_{s-p} component was negligibly small in the region of phase II, we suggest that a tightly packed structure is formed, in which the molecular hyperpolarizability is directed roughly normal (perpendicular) to the water surface.

The SHG profile of Ru2C16B was quite different from that of Ru4C16B. As shown in Figure 4, the SHG signal rose almost synchronously with the rise of surface pressure. A somewhat sudden increase of the I_{p-p} component was observed almost as soon as compression was begun; then, after a "plateau" period during which the SHG intensity was unchanged, it increased again roughly monotonically with further compression (Figure 4a). The signal for the I_{s-p} component, on the other hand,

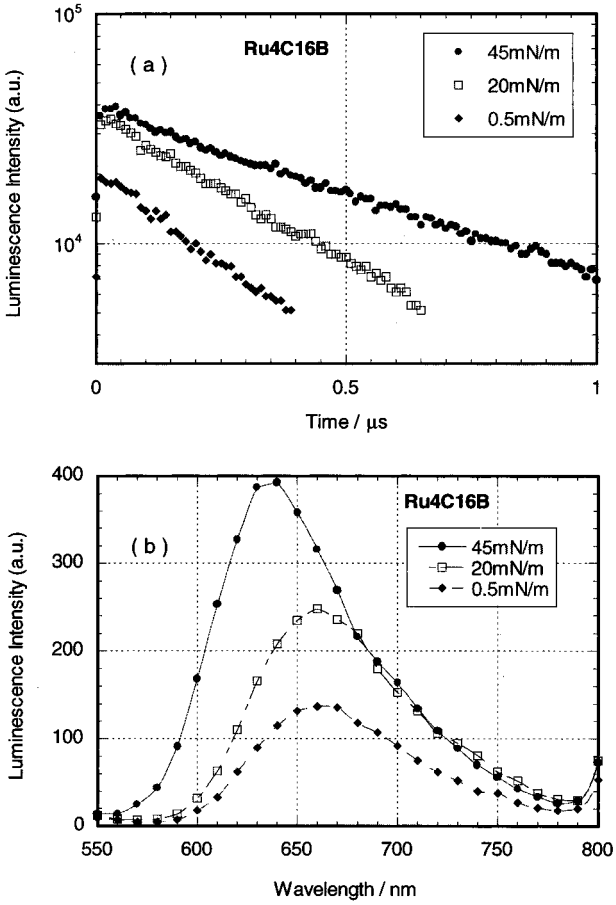

Figure 5. Luminescence spectra (a) and lifetimes (b) of Ru4C16B monolayer assembly at the air/water interface for various surface pressures.

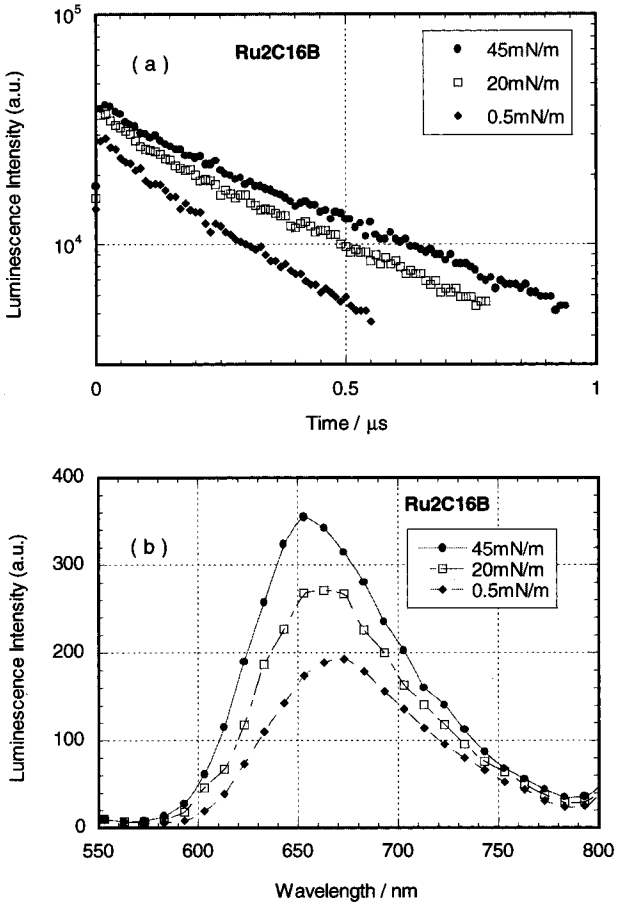

Figure 6. Luminescence spectra (a) and lifetimes (b) of Ru2C16B monolayer assembly at the air/water interface for various surface pressures.

increased very steeply at first but did not change significantly with additional compression (Figure 4b). The appearance of the I_{s-p} component means the generation of a perpendicular component of noncentrosymmetric polarization with reference to the water surface. These results indicate that the aggregated Ru2C16B becomes ordered quickly and that the degree of ordering becomes higher with continued compression. In Ru2C16B, the size of the hydrophilic headgroup is larger than that of the cross section of the hydrophobic part composed of two *n*-hexadecyl groups. Thus, the hydrophilic headgroups impose packing constraints in the Ru2C16B monolayer.

In each complex, the luminescence signal increased with increasing surface pressure because the number density of the complex increased as the monolayer was compressed. Luminescence spectra and lifetimes of each complex were measured at 0.5, 20, and 45 mN/m as typical points; the results are shown in Figure 5 for Ru4C16B and in Figure 6 for Ru2C16B. In both complexes, the luminescence intensity increased, its peak shifted to a shorter-wavelength region, and the lifetime became longer at higher surface pressures. In the case of Ru4C16B, a remarkable blue-shift (~25 nm) and increased lifetime were observed on going from 20 mN/m (0.3 μs) to 45 mN/m (0.6 μs). These observations indicate that some densely packed structures are formed in the phase II region and the motion of the headgroups is highly restricted. Thus, dense packing in phase II is imposed by the pendant four *n*-hexadecyl groups.

With Ru2C16B, on the other hand, the extent of the increase in luminescence upon compression from 0.5 to 45 mN/m is reasonable, judging from the increase in the molecular density. A red-shift of the luminescence peak in Ru2C12B (in which the hexadecyl groups of Ru2C16B are replaced by dodecyl groups) has been observed with the increase of water content in reversed micellar systems (aerosol OT).[18] These results suggest that, in the phase II region, collisional quenching is hindered because of dense packing.

In conclusion, we have continuously measured the in-situ SHG and luminescence signals of monolayer assemblies of two amphiphilic ruthenium complexes at the air/water interface as a function of molecular area. The monolayer structures observed were quite dependent on the number of aliphatic tails. The four-tailed complex could accommodate tight aggregation at higher surface pressures, imposed by the pendant aliphatic tails. Comparisons of the present results at the air/water interface with the behavior of transferred LB films should be very interesting, and this work is in progress.

Acknowledgment. We thank Dr. Y. Niidome and Mr. H. Ayukawa for their cooperation in the measurements. The present study was partially supported by the Grant-in-Aid for Scientific Research on Priority Areas (no. 09222218).

References and Notes

(1) Fukuda, K.; Sugi, M. *Langmuir−Blodgett Films 4*, Vol. 1; Elsevier Applied Science: New York, 1989.
(2) Shen, Y. R. *Nature* **1989**, *337*, 519.
(3) Eisenthal, K. B. *Acc. Chem. Res.* **1993**, *26*, 636.
(4) Eisenthal, K. B. *Chem. Rev.* **1996**, *96*, 1343.
(5) Corn, R. M.; Higgins, D. A. *Chem. Rev.* **1994**, *94*, 107.
(6) Rasing, T.; Shen, Y. R.; Kim, M. K.; Grubb, S. *Phys. Rev. Lett.* **1985**, *55*, 2903.
(7) Rasing, T.; Shen, Y. R.; Kim, M. W.; Valint, P.; Bock, J. *Phys. Rev. A* **1985**, *31*, 537.
(8) Groh, W.; Lupo, D.; Sixl, H. *Angew. Chem. Adv. Mater.* **1989**, *101*, 1580.

(9) Berkovic, G.; Rasing, Th.; Shen, Y. R. *J. Opt. Soc. Am. B* **1988**, *4*, 1580.

(10) Huang, J.; Lewis, A.; Rasing, T. *J. Phys. Chem.* **1988**, *92*, 1756.

(11) Shirota, K.; Kajikawa, K.; Takezoe, H.; Fukuda, A. *Jpn. J. Appl. Phys.* **1990**, *29*, 750.

(12) Verbiest, T.; Samyn, C.; Persoons, A. *Thin Solid Films* **1994**, *242*, 139.

(13) Ahuja, R. C.; Matsumoto, M.; Möbius, D. *J. Phys. Chem.* **1992**, *96*, 1855.

(14) Yamada, S.; Nakano, T.; Matsuo, T. *Thin Solid Films* **1994**, *245*, 196.

(15) Sakaguchi, H.; Nakamura, H.; Nagamura, T.; Ogawa, T.; Matsuo T. *Chem. Lett*. **1989**, 1715.

(16) Matsuo, T.; Takuma, K.; Tsutsui, Y.; Nishijima, T. *J. Coord. Chem.* **1980**, *10*, 187.

(17) Heinz, T. F.; Tom, H. W. K.; Shen, Y. R. *Phys. Rev. Lett.* **1983**, *28*, 1883.

(18) Kaizu, Y.; Ohta, H.; Kobayashi, K.; Kobayashi, H.; Takuma, K.; Matsuo, T. *J. Photochem.* **1985**, *30*, 93.